International Journal of Control

ISSN: 0020-7179 (Print) 1366-5820 (Online) Journal homepage: www.tandfonline.com/journals/tcon20

Smith predictor design for robust performance

DANIEL L. LAUGHLIN, DANIEL E. RIVERA & MANFRED MORARI

To cite this article: DANIEL L. LAUGHLIN, DANIEL E. RIVERA & MANFRED MORARI (1987) Smith predictor design for robust performance, International Journal of Control, 46:2, 477-504, DOI: 10.1080/00207178708933912

To link to this article: https://doi.org/10.1080/00207178708933912

INT. J. CONTROL, 1987, VOL. 46, NO. 2, 477–504

Smith predictor design for robust performance

DANIEL L. LAUGHLIN†, DANIEL E. RIVERA† and
MANFRED MORARI†

A method is outlined for designing Smith predictor controllers that provide robust performance despite real parameter uncertainties in the process model. Insight into the design process is gained by viewing the Smith predictor from the perspective of internal model control. Performance requirements are written in terms of a frequency-domain weight restricting the magnitude of the closed-loop sensitivity function. A general method for approximating multiple parameter uncertainties by a single multiplicative uncertainty is developed—an exact bound is derived for the magnitude of multiplicative uncertainty used to approximate simultaneous uncertainties in process gain, time-constant, and time-delay. Three different tuning methods are demonstrated; each is applied to a wide range of parameter uncertainties in a first-order with time-delay model. The first tuning method locates loop transfer-function uncertainty regions to test for robust performance—real parameter uncertainties are considered exactly. The second tuning method approximates real parameter uncertainties by multiplicative uncertainty and uses structured singular value analysis to guarantee robust performance. The third is a 'quick design' method that considers the unit magnitude crossing of the multiplicative uncertainty. Finally, the Smith predictor controller is compared with the structured-singular-value-optimal controller.

1. Introduction

Callender *et al.* (1936) recognized the importance of time-lag in a control system more than fifty years ago. In the last five decades their 'controlling gear' and 'control apparatus' has given way to high speed digital computers, but the basic problem remains the same: robust controllers must be designed for systems with time-delay. In particular, the chemical process industries require controllers that can cope with material transport delays, composition analysis delays and other delays that cannot be avoided.

1.1. *Smith predictors*

Early researchers addressed the problem of controller design for systems with time-delay by correlating PID controller settings with model gain, time-constants and time-delay (e.g. Cohen and Coon 1953). Low loop gains were required to avoid instability when time-constants were small compared to the time-delay, leading to poor system performance. Smith enabled larger loop gains to be used by incorporating a minor feedback loop around a conventional controller (see Fig. 1) to stabilize the system (Smith 1957). The effect of the minor feedback loop has been described as similar to that of a lead network with considerable lead (Åström 1977). The Smith predictor controller has been particularly successful in tracking step commands when applied to systems with the ability to respond quickly (systems with small time-constants) despite large time-delays between the controller and the plant input

Received 9 September 1986. Revised 31 October 1986.
† Chemical Engineering 206-41, CALTECH, Pasadena, CA 91125, U.S.A.

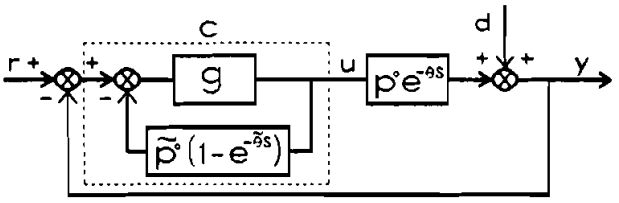

Figure 1. The Smith predictor control structure. A conventional controller g and a minor feedback loop are used to control systems with time-delay.

(Horowitz 1983). In the absence of modelling error the Smith predictor has been shown to lead to optimal response to step disturbances. Although first suggested for use in single-input–single-output (SISO) systems, the Smith predictor concept for controlling systems with time-delay has been extended to multivariable systems (e.g. Holt 1984, Palmor 1985, Bhaya and Desoer 1985, Jerome and Ray 1986).

1.2. *Robust performance for systems with time-delay*

Only recently have researchers attempted to quantify the Smith predictor controller's robustness to modelling errors. In several studies stability boundaries were plotted as functions of error in a single plant parameter (Ioannides *et al.* 1979, Palmor 1980, Palmor and Shinnar 1981). Brosilow (1979) proposed a method for tuning the Smith predictor when one model parameter was uncertain: either gain, time-constant, or time-delay. Owens and Raya (1982) consider the effect of additive plant/model mismatch on the robust stability of Smith predictor controllers and derive an expression for a bound on the magnitude of multiplicative uncertainty used to approximate time-delay uncertainty. All these studies failed to consider the effect of *simultaneous* uncertainties in gain, time-constant, and time-delay on the robustness of Smith predictors. Finally, Chen (1984) addressed this failure by locating regions on the complex plane corresponding to first-order models with uncertain gain, time-constant, and time-delay. Chen correctly evaluated *robust stability* of Smith predictor controllers using these regions. The question of *robust performance* of Smith predictor controllers despite simultaneous parameter uncertainties remained unanswered.

The research results presented here address the question of robust performance of Smith predictor controllers. A systematic design procedure is presented that will guarantee robust Smith predictors despite uncertainties in model parameters. Specific results include:

(1) a concise method for designing robust Smith predictor controllers with a single tuning parameter;

(2) a method for tuning the controllers for robustness with respect to simultaneous uncertainties in gain, time-constant, and time delay or with respect to uncertainty in an even greater number of model parameters; and

(3) a rigorous test for robust performance with respect to parameter uncertainties.

2. Modelling uncertainty in processes with time-delay

It is often convenient to model processes with transfer-functions containing real-parameter uncertainties as in

$$\Pi' = \left\{ p(s) \,|\, p(s) = p'(s) \left[\frac{a_n s^n + a_{n-1} s^{n-1} + \ldots + a_1 s + a_0}{b_m s^m + b_{m-1} s^{m-1} + \ldots + b_1 s + b_0} \right] \exp(-\theta s) \right\} \qquad (1)$$

$$a_i \in [a_{i_{\min}}, a_{i_{\max}}], \quad b_i \in [b_{i_{\min}}, b_{i_{\max}}], \quad \theta \in [\theta_{\min}, \theta_{\max}]$$

or

$$\Pi' = \left\{ p(s) \,|\, p(s) = p'(s) \left[\frac{k \Pi_i ((1/z_i)s + 1)}{\Pi_i ((1/p_i)s + 1)} \right] \exp(-\theta s) \right\} \tag{2}$$

$$z_i \in [z_{i_{\min}}, z_{i_{\max}}], \quad p_i \in [p_{i_{\min}}, p_{i_{\max}}], \quad k \in [k_{\min}, k_{\max}], \quad \theta \in [\theta_{\min}, \theta_{\max}]$$

For example, the parameter bounds may represent uncertain process flow rates, uncertainty introduced by linearizing a model at different steady states or variations in environmental operating conditions (temperature, pressure, relative humidity, etc.). The factor $p'(s)$ in (1) and (2) is known exactly and does not contain parameter uncertainties. A special case of (1) and (2) is the popular first-order with time-delay model (3).

$$\Pi' = \left\{ p(s) \,|\, p(s) = p'(s) \frac{k \exp(-\theta s)}{\tau s + 1} \right\} \tag{3}$$

$$k \in [k_{\min}, k_{\max}], \quad \tau \in [\tau_{\min}, \tau_{\max}], \quad \theta \in [\theta_{\min}, \theta_{\max}]$$

The model (3) has been used extensively to describe chemical processes. Time-delay is often used in the simple model to incorporate additional phase-lag caused by ignored higher-order dynamics or to approximate the dynamics of a distributed parameter system. For example, Ogunnaike (1986) uses (3) to represent almost every element in a multivariable model for a distillation column.

The method proposed in this paper for designing robust Smith predictor controllers applies to all models (1) and (2) that are open-loop stable. The particular case (3) with simultaneous uncertainties in gain, time-constant, and time-delay will be studied in detail. Controller parameters leading to robust performance for various levels of uncertainty in these three parameters will be presented.

2.1. *Locating model uncertainty regions from parameter uncertainties*

The set of possible process models indicated by (1)–(3) can be represented at each frequency by a simply connected region $\pi(\omega)$ on the complex plane. A method has been developed for locating the regions $\pi(\omega)$ corresponding to the transfer functions in equation (1) with any required degree of accuracy (Laughlin *et al.* 1986). East (1981, 1982) outlined a conservative method for locating convex polygons containing regions corresponding to (2) when the time-delay is known exactly. A set Π of all possible process models can be defined as follows:

$$\Pi = \{ p(s) \,|\, p(i\omega) \in \pi(\omega), \quad \forall \omega \} \tag{4}$$

The set Π given by (4) is almost always larger than the corresponding set Π' given by (1)–(3) since some elements of Π might not be expressed by a transfer-function with the specified structure. To prove robustness requirements are met for all models in (1)–(3) it is sufficient to show that they are met for all models in the corresponding set Π.

2.2. *Translating parameter uncertainty into multiplicative error*

When modelling error is represented by uncertainty in several real parameters it is often mathematically convenient to approximate the uncertainty with a single multiplicative perturbation. Multiplicative perturbations on a nominal plant are represented by (5).

$$p(s) = \tilde{p}(s)[1 + l_m(s)], \quad |l_m(i\omega)| < l(\omega) \tag{5}$$

Using the norm-bounded multiplicative error $l_m(s)$ is equivalent to representing process uncertainty by a disc-shaped uncertainty region $\pi(\omega)$ with radius $|\tilde{p}(i\omega)|l(\omega)$ on the complex plane. The multiplicative uncertainty description can be incorporated into controller optimization techniques where parameter uncertainty descriptions are less tractable.

It is straightforward to determine the bound $l(\omega)$ on the magnitude of the multiplicative error for the general cases of parameter uncertainty (1) and (2). First the boundaries of a sufficient number of uncertainty regions $\pi(\omega)$ must be located over the frequency range of interest. Next a nominal model $\tilde{p}(i\omega)$ must be specified—in the proposed design procedure parameters will be fixed at their mean values in the nominal model. Finally the maximum distance $d(\omega)$ from $\tilde{p}(i\omega)$ to any point on the boundary of $\pi(\omega)$ is determined at each frequency. This distance $d(\omega)$ is related to the bound on the magnitude of the multiplicative error through $d(\omega) = |\tilde{p}(i\omega)|l(\omega)$.

For the special case of simultaneous uncertainties in gain, time-constant and time-delay in the first-order model (3), an exact analytical expression for the bound $l(\omega)$ can be derived. Owens and Raya (1982) derived the simple expression $l(\omega) = |\exp(\Delta\theta i\omega) - 1|$ for the bound when only uncertainties in time-delay are considered. Bound 1 specifies the smallest possible magnitude $|l_m(i\omega)| = l(\omega)$ such that all plants given by (3) with *simultaneous* errors in gain, time-constant and time-delay can be represented by $p(s) = \tilde{p}(s)[1 + l_m(s)]$.

Bound 1: *Gain, time-delay and pole uncertainty*

Consider the following set of process models:

$$p(s) = p'(s)\frac{(\bar{k} + \delta k)\exp[-(\bar{\theta} + \delta\theta)s]}{(\bar{\tau} + \delta\tau)s + 1} \tag{6}$$

where $p'(s)$ does not contain parameter uncertainties and $\bar{k}$, $\bar{\tau}$, $\bar{\theta}$, δk, $\delta\tau$ and $\delta\theta$ are defined by:

$$\bar{k} = \frac{k_{min} + k_{max}}{2}, \quad \bar{\tau} = \frac{\tau_{min} + \tau_{max}}{2}, \quad \bar{\theta} = \frac{\theta_{min} + \theta_{max}}{2}$$

$$|\delta k| \leqslant \Delta k = |k_{max} - \bar{k}| < |\bar{k}|, \quad |\delta\tau| \leqslant \Delta\tau = |\tau_{max} - \bar{\tau}| < |\bar{\tau}|, \quad |\delta\theta| \leqslant \Delta\theta = |\theta_{max} - \bar{\theta}| < |\bar{\theta}|$$

Define a nominal model $\tilde{p}(s)$ with gain, time-constant and time-delay at their mean values:

$$\tilde{p}(s) = p'(s)\frac{\bar{k}\exp(-\bar{\theta}s)}{\bar{\tau}s + 1} \tag{7}$$

The smallest possible bound $l(\omega)$ on the multiplicative error $l_m(s)$ such that all models in (6) are contained in the set $p(s) = \tilde{p}(s)[1 + l_m(s)]$, $|l_m(i\omega)| < l(\omega)$, is given by:

$$l(\omega) = \left|\left(\frac{|\bar{k}| + \Delta k}{|\bar{k}|}\right)\left(\frac{\bar{\tau}i\omega + 1}{(\bar{\tau} \mp \Delta\tau)i\omega + 1}\right)\exp(\pm\Delta\theta i\omega) - 1\right|, \quad \forall\,\omega < \omega^* \tag{8}$$

$$l(\omega) = \left|\left(\frac{|\bar{k}| + \Delta k}{|\bar{k}|}\right)\left(\frac{\bar{\tau}i\omega + 1}{(\bar{\tau} \mp \Delta\tau)i\omega + 1}\right)\right| + 1, \quad \forall\,\omega \geqslant \omega^* \tag{9}$$

where ω^* is defined implicitly by:

$$\pm\Delta\theta\omega^* + \arctan\left[\frac{\pm\Delta\tau\omega^*}{1 + \bar{\tau}(\bar{\tau} \mp \Delta\tau)\omega^{*2}}\right] = \pm\pi, \quad \frac{\pi}{2} \leqslant \Delta\theta\omega^* \leqslant \pi \tag{10}$$

Bound 1 applies to both stable and unstable models (6). Top signs are selected in (8)–(10) if $\bar{\tau}$ is positive indicating a left-half-plane pole. Bottom signs are selected in (8)–(10) if $\bar{\tau}$ is negative indicating a right-half-plane pole. Note that Bound 1 simplifies to the expression derived by Owens and Raya (1982) when $\Delta k = \Delta\tau = 0$. Proof of Bound 1 is given in the appendix along with a similar bound on multiplicative error for the case of simultaneous variations in gain, time-delay and one process zero location. The bounds $l(\omega)$ for $\Delta k/\bar{k} = \Delta\tau/\bar{\tau} = \Delta\theta/\bar{\theta} = 0{\cdot}1$ and for $\Delta k/\bar{k} = \Delta\tau/\bar{\tau} = \Delta\theta/\bar{\theta} = 0{\cdot}5$ are shown in Fig. 2.

3. Selecting performance requirements

3.1. *Robust stability*

The standard feedback control structure is shown in Fig. 3 with commands $r(s)$, disturbances $d(s)$, outputs $y(s)$, control actions $u(s)$ and errors $e(s)$. The control structure must be stable for all process models in the set Π. Once a controller $c(s)$ is selected, robust stability can be evaluated with respect to the actual parameter uncertainties or with respect to the multiplicative uncertainty approximation. When considering the actual parameter uncertainties the closed-loop system is stable for all plants in Π if and only if a nominal system with $p(s) = \tilde{p}(s) \in \Pi$ is stable and the regions $\pi(\omega)c(i\omega)$ exclude $(-1, 0)$ for all frequencies ω. When the modelling error is described in terms of a multiplicative uncertainty as in (5), robust stability is guaranteed if and only if a nominal system with $p(s) = \tilde{p}(s) \in \Pi$ is stable and

$$|\tilde{h}(i\omega)|l(\omega) < 1, \quad \forall\,\omega \tag{11}$$

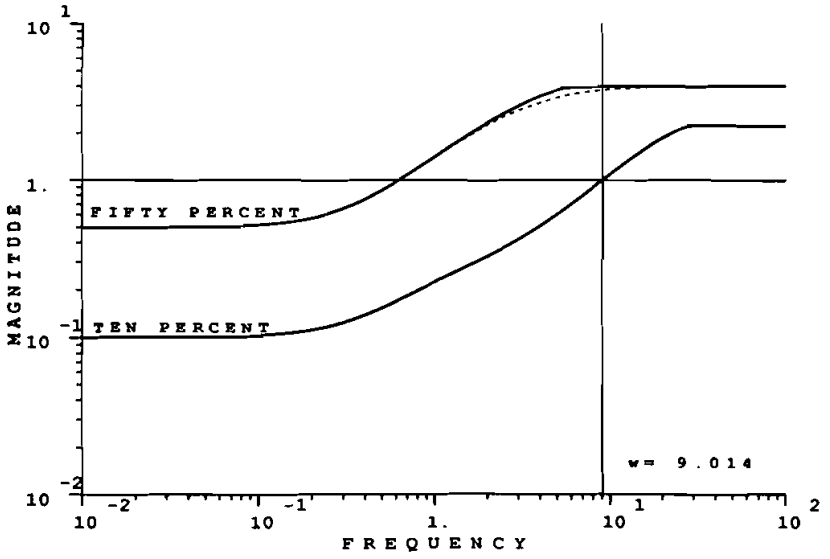

Figure 2. The bound $l(\omega)$ on the magnitude of the multiplicative uncertainty is shown for both 10 per cent parameter uncertainty and 50 per cent parameter uncertainty in model (6). At a frequency of 9·014 rad s^{-1} the bound $l(\omega) = 1{\cdot}0$ for the case of 10 per cent parameter uncertainty. The dashed curve is the magnitude of the rational function

$$l_m(s) = 1{\cdot}5\left(\frac{s+1}{0{\cdot}5s+1}\right)\left(\frac{1+0{\cdot}25s}{1-0{\cdot}25s}\right) - 1$$

used to approximate the bound $l(\omega)$ for SSV-optimal controller synthesis.

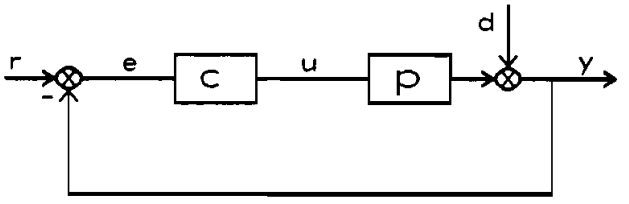

Figure 3. The standard feedback control structure with commands $r(s)$, disturbances $d(s)$, outputs $y(s)$, control actions $u(s)$ and errors $e(s)$.

where the nominal complementary sensitivity function $\tilde{h}(i\omega)$ is given by

$$\tilde{h}(i\omega) = \frac{\tilde{p}(i\omega)c(i\omega)}{1 + \tilde{p}(i\omega)c(i\omega)}$$

Condition (11) is equivalent to the condition that the disc-shaped regions with radius $|\tilde{p}(i\omega)c(i\omega)|l(\omega)$ centred at $\tilde{p}(i\omega)c(i\omega)$ exclude $(-1, 0)$ for all frequencies ω.

3.2. *Robust performance*

In addition to robust stability, 'good' command-following and disturbance-rejection are required of the control structure in Fig. 3. If the error signal $e(t) = r(t) - y(t)$ is kept 'small' for all inputs $r(t) - d(t)$, these performance objectives can be met. The errors are related to the inputs as shown in (12).

$$\frac{e(i\omega)}{r(i\omega) - d(i\omega)} = \frac{1}{1 + p(i\omega)c(i\omega)} \tag{12}$$

In this study robust performance will be defined mathematically by placing a bound on the magnitude of the sensitivity function $s(i\omega) = [1 + p(i\omega)c(i\omega)]^{-1}$.

$$|s(i\omega)| = \left|\frac{1}{1 + p(i\omega)c(i\omega)}\right| < \left|\frac{1}{w_2(i\omega)}\right|, \quad \forall\,\omega, \forall\, p(s) \in \Pi \tag{13}$$

Usually only small steady-state errors are acceptable so the magnitude of the performance weight $|w_2(i\omega)|$ is specified to be large at low frequencies and small at high frequencies. The inverse of a typical weight is shown in Fig. 4. For convenience (13) can be written as:

$$|1 + p(i\omega)c(i\omega)| > |w_2(i\omega)|, \quad \forall\,\omega, \forall\, p(s) \in \Pi \tag{14}$$

Since all plants $p(s) \in \Pi$ are restricted to lie within region $\pi(\omega)$ at frequency ω, the requirement (14) can be met by ensuring that the distance of regions $\pi(\omega)c(i\omega)$ from $(-1, 0)$ is greater than $|w_2(i\omega)|$.

When $p(i\omega) = \tilde{p}(i\omega)[1 + l_m(i\omega)]$, $|l_m(i\omega)| < l(\omega)$, (14) can be written in terms of the nominal complementary sensitivity function $\tilde{h}(i\omega) = 1 - \tilde{s}(i\omega)$ as follows:

$$\sup_{\omega} |\tilde{h}(i\omega)|l(\omega) + |(1 - \tilde{h}(i\omega))w_2(i\omega)| < 1 \tag{15}$$

Given nominal stability, both robust stability and robust performance of the control system are guaranteed if and only if condition (15) is satisfied. Condition (15) represents an additional performance specification for the complementary sensitivity function $\tilde{h}(i\omega)$ beyond the small gain theorem requirement (11) for robust stability alone.

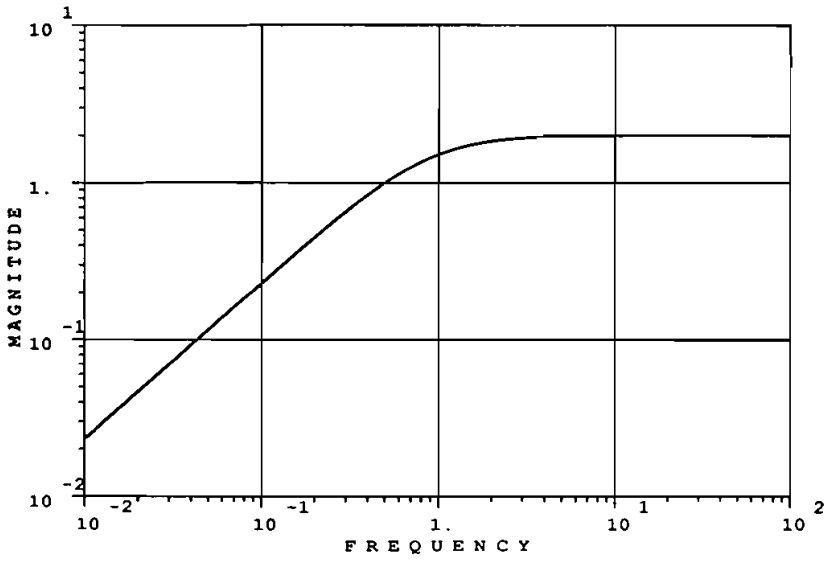

Figure 4. The inverse of the performance weight $w_2(s) = (1{\cdot}162s + 1)/2{\cdot}324s$ used for experiment 1 in Table 5. The worst-case sensitivity function must lie below this curve to satisfy the robust performance specification.

Requirement (15) is equivalent to a special case of the robust performance condition derived by Doyle (1982). Doyle defines the 'structured singular value' to be the supremum in (15).

3.3. *A performance weight for the Smith predictor problem*

Performance requirement (13) indicates that the weight $w_2(s)$ specifies a bound on the maximum peak of the sensitivity function. It is useful to examine the functional form of the H_2-optimal nominal sensitivity function for the expected inputs before selecting a performance weight for a particular problem. An expression for the H_2-optimal nominal sensitivity function for general inputs is given by the theorem in § 4.2 of this paper. If the process were known exactly the weight $w_2(s)$ could be selected to be just less than the inverse of the nominal sensitivity function. This would lead to a structured singular value for the system of just less than one; the system would pass the robust performance test.

For the special case of first-order with time-delay systems (3) the H_2-optimal nominal sensitivity function for step inputs is:

$$\tilde{s}_{\text{opt}}(i\omega) = 1 - \exp(-\bar{\theta} i\omega) \tag{16}$$

If a first-order Padé approximation is used for the time-delay in (16) equation (17) results.

$$\tilde{s}_{\text{opt}}(i\omega) \approx \frac{\bar{\theta} i\omega}{\frac{\bar{\theta}}{2} i\omega + 1} \tag{17}$$

Equation (17) suggests the following functional form for the weight $w_2(i\omega)$:

$$w_2(i\omega) = b\frac{ai\omega + 1}{ai\omega} \tag{18}$$

Note expressions (17) and (18) are inverses of one another when $a = \bar{\theta}/2$ and $b = 1/2$. The weight $w_2(i\omega)$ in (18) requires that the bandwidth of the closed-loop system be at least $1/a$ and that the maximum peak in the sensitivity function be less than $1/b$. Parameter a would be increased and parameter b decreased to allow for degradation in closed-loop performance due to modelling errors. The inverse of the weight $w_2(i\omega)$ used for experiment 1 in Table 5 with $a = 1{\cdot}162$ and $b = 0{\cdot}5$ is sketched in Fig. 4. The worst-case (largest magnitude) sensitivity function generated by the set of models Π must lie below this curve to satisfy the robust performance specification. The controller is typically designed to push the worst-case sensitivity function as far below this curve as possible over the entire frequency range.

4. Designing the controller

4.1. *Smith predictor structure*

In order to construct the Smith predictor control structure shown in Fig. 1 it is necessary to select a process model $\tilde{p}(s) = \tilde{p}^0(s) \exp(-\tilde{\theta}s)$ and to design the controller $g(s)$. Usually $g(s)$ is selected to be a conventional P, PI or PID controller. The controller $g(s)$ must be designed so that the system is robust with respect to errors between the actual process $p^0(s) \exp(-\theta s)$ and the model $\tilde{p}^0(s) \exp(-\tilde{\theta}s)$.

The Smith predictor control structure can be considered to be a particular parameterization of the more general feedback control structure. The relationship between $g(s)$ and the standard feedback controller $c(s)$ in Fig. 3 is given by (19).

$$c(s) = \frac{g(s)}{1 + g(s)\tilde{p}^0(s)[1 - \exp(-\tilde{\theta}s)]} \tag{19}$$

Unfortunately, the Smith predictor structure does not provide much insight into the design of controller $g(s)$. The effect of the level of model uncertainty on the choice of controller parameters is not clear. A systematic method for designing robust Smith predictors can be developed by considering an alternate parameterization of the controller.

4.2. *Internal model control parameterization of the Smith predictor*

An alternate parameterization of $c(s)$ is the internal model control (IMC) structure shown in Fig. 5. It has been shown that the IMC structure leads to a Smith predictor controller for open-loop stable processes with time-delay (Brosilow 1979, Holt 1984, Rivera *et al.* 1985). An advantage of the IMC structure is that the system is guaranteed to be nominally stable if both $\tilde{p}(s)$ and $q(s)$ are stable (Garcia and Morari 1982). Moreover, since any transfer function (e.g. $\tilde{h}(s) = \tilde{p}(s)q(s)$) relating inputs to outputs is

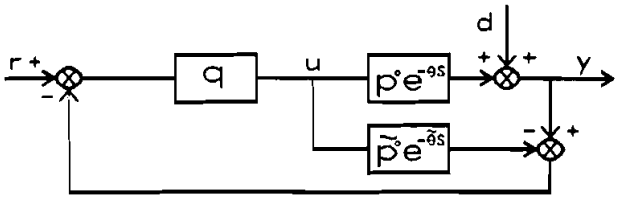

Figure 5. The internal model control (IMC) parameterization of the Smith predictor controller.

affine in the IMC controller the restrictions placed on $q(s)$ by robustness requirements (11) and (15) are clear. Usually only a single tuning parameter λ is required. Adjusting λ to meet stability and performance requirements is straightforward.

The IMC design procedure involves two steps:

(1) a controller $\tilde{q}(s)$ is designed to be H_2-optimal for the nominal model and the expected input to the system; and

(2) the controller is 'detuned' by the addition of a low-pass filter $f(s)$ to meet robustness requirements.

The resulting IMC controller is given by $q(s) = \tilde{q}(s)f(s)$.

Morari *et al.* (1987) derived the following theorem for the H_2-optimal controller $\tilde{q}(s)$ when $\tilde{p}(s)$ is stable.

Theorem

Consider the IMC structure shown in Fig. 5 with process model $\tilde{p}(s)$ and controller $q(s)$. The nominal model $\tilde{p}(s)$ is factored into an allpass portion $\tilde{p}_A(s)$ and a minimum phase portion $\tilde{p}_M(s)$

$$\tilde{p}(s) = \tilde{p}_A(s)\tilde{p}_M(s)$$

so that $\tilde{p}_A(s)$ includes all the right-half-plane zeros and delays of $\tilde{p}(s)$ and

$$|\tilde{p}_A(i\omega)| = 1, \quad \forall\, \omega$$

The expected disturbance input $d(s)$ is factored similarly

$$d(s) = d_A(s)d_M(s)$$

The controller $\tilde{q}(s)$ that minimizes the two-norm of the error is then given by

$$\tilde{q}(s) = (\tilde{p}_M(s)d_M(s))^{-1}[\tilde{p}_A^{-1}(s)d_M(s)]_* \tag{20}$$

where the operator $[\,\cdot\,]_*$ denotes that after a partial fraction expansion of the operand all terms involving the poles of $\tilde{p}_A^{-1}(s)$ are omitted. The H_2-optimal sensitivity function $\tilde{s}(i\omega)$ is given by

$$\tilde{s}(i\omega) = 1 - \tilde{p}(i\omega)q(i\omega) = 1 - \tilde{p}_A(i\omega)\tilde{d}_M^{-1}(i\omega)[\tilde{p}_A^{-1}(i\omega)d_M(i\omega)]_*$$

The filter form is selected to ensure that the controller $q(s)$ is proper and that the closed-loop system has the appropriate asymptotic tracking properties. For asymptotic tracking of step inputs $f(s)$ can be chosen of the form

$$f(s) = \frac{1}{(\lambda s + 1)^n}$$

where n is large enough to make $q(s)$ proper and λ is the IMC filter tuning parameter. (Filter forms for other inputs can be found in Morari *et al.* 1987.) Usually a single tuning parameter is used. A small value for λ yields faster system response whereas a large λ detunes the system and results in greater stability margins. If robust performance is specified in terms of a weight like $w_2(i\omega)$ in (18) with both bandwidth and maximum peak (MP) requirements, it may not be possible to meet both requirements with a single tuning parameter. When confronted with this situation the filter form can be changed to incorporate more tuning parameters as in

$$f(s) = \frac{1}{(\lambda_1 s + 1)(\lambda_2 s + 1)}$$

or an alternative constant performance weight $w_2' = 1/MP$ without a bandwidth constraint can be selected. If the alternative weight is selected the controller is designed so that the maximum magnitude of the sensitivity function is equal to $1/w_2' = MP$. Designing the controller so that the worst-case sensitivity function is as far below $1/w_2' = MP$ has no meaning since the absence of a bandwidth requirement in w_2' would allow complete detuning of the controller ($\lambda = \infty$ and $c(s) = 0$).

The relationship between the IMC controller $q(s)$ and the standard feedback controller $c(s)$ is given by (21).

$$c(s) = \frac{q(s)}{1 - q(s)\tilde{p}^0(s)\exp(-\bar{\theta}s)} \tag{21}$$

The particular example of controller design for first-order with time-delay systems clarifies the relationship between the IMC parameterization and the Smith predictor. Consider the set of process models (6) with $p' = 1$. Select the nominal model as in (7) with all parameters at their mean values. The H_2-optimal controller $\tilde{q}(s)$ for step disturbances is given by $\tilde{q}(s) = (\bar{\tau}s + 1)/\bar{k}$. The appropriate filter is $f(s) = 1/(\lambda s + 1)$, resulting in the IMC controller

$$q(s) = \frac{\bar{\tau}s + 1}{\bar{k}(\lambda s + 1)} \tag{22}$$

Substituting the IMC controller (22) and the nominal model (7) into the expression (21) for the conventional feedback controller results in

$$c(s) = \frac{\bar{\tau}s + 1}{\bar{k}(\lambda s + 1 - \exp(-\bar{\theta}s))} \tag{23}$$

Note that (23) is equivalent to the Smith predictor controller (19) when $\tilde{p}^0(s) = \bar{k}/(\bar{\tau}s + 1)$ and $g(s)$ is the PI controller $g(s) = (\bar{\tau}s + 1)/\bar{k}\lambda s$.

5. Tuning the controller for robust performance

In this section five alternative methods are presented for designing robust controllers for systems with time-delay. The first four methods result in Smith predictor controllers; the fifth, in the structured-singular-value-optimal controller. The methods differ in their numerical complexity, in the type of uncertainty description they consider, and in the robust performance guarantee they offer. The more numerically complex methods introduce less conservativeness into the controller design. In selecting an appropriate design method the required system performace is of paramount importance. If performance requirements are mild then the 'quick design' procedure should suffice. Moderate performance requirements might necessitate the robustness test that considers actual parameter uncertainties rather than a multiplicative error approximation. More demanding performance requirements might require optimizing all parameters in the Smith predictor controller. Only the toughest performance requirements would justify synthesis of the structured-singular-value-optimal controller.

The IMC design procedure and tuning methods presented here are applicable to all open-loop stable processes that can be modelled by (1) or (2). The methods are illustrated with controller designs for the particularly useful first-order with time-delay model. Three recommended tuning methods were compared by examining controller designs for twenty-four families of process models (3) with $p'(s) = 1$. All

possible combinations of 10 per cent and 50 per cent uncertainty in gain, time-constant and time-delay were investigated at each of three levels of the ratio $\bar{\tau}/\bar{\theta}$. Tuning method A was used to design controllers for an even greater range of the parameter uncertainties and the ratio $\bar{\tau}/\bar{\theta}$. The results of the different IMC filter-tuning techniques are presented in Tables 1–5. Details of each of the tuning techniques are outlined below.

Experiment	$dk/\bar{k}$	$d\tau/\bar{\tau}$	$d\theta/\bar{\theta}$	λ robust stability	For MP = 2·0		
					λ_A	λ_B	λ_C
1	0·1	0·1	0·1	0·080	0·525	0·661	0·313
2	0·1	0·5	0·1	0·230	1·109	1·647	1·425
3	0·5	0·1	0·1	0·107	1·199	1·498	0·495
4	0·1	0·1	0·5	0·401	1·136	1·648	1·594
5	0·1	0·5	0·5	0·737	1·412	2·547	2·895
6	0·5	0·5	0·1	0·627	1·833	2·677	3·135
7	0·5	0·1	0·5	0·537	2·012	2·256	2·367
8	0·5	0·5	0·5	1·091	2·312	3·477	4·541

Table 1. Filter parameters resulting from tuning methods A–C. λ from robust stability condition is shown for comparison. In experiments 1–8 the ratio $\bar{\tau}/\bar{\theta} = 1·0$.

Experiment	$dk/\bar{k}$	$d\tau/\bar{\tau}$	$d\theta/\bar{\theta}$	λ robust stability	For MP = 2·0		
					λ_A	λ_B	λ_C
9	0·1	0·1	0·1	0·080	0·454	0·632	0·316
10	0·1	0·5	0·1	0·185	0·758	1·172	0·923
11	0·5	0·1	0·1	0·107	1·115	1·344	0·496
12	0·1	0·1	0·5	0·399	1·104	1·608	1·562
13	0·1	0·5	0·5	0·611	1·189	2·087	2·208
14	0·5	0·5	0·1	0·367	1·293	1·872	1·733
15	0·5	0·1	0·5	0·529	1·998	2·120	2·202
16	0·5	0·5	0·5	0·823	2·125	2·704	3·194

Table 2. Filter parameters resulting from tuning methods A–C. λ from robust stability condition is shown for comparison. In experiments 9–16 the ratio $\bar{\tau}/\bar{\theta} = 0·5$.

Experiment	$dk/\bar{k}$	$d\tau/\bar{\tau}$	$d\theta/\bar{\theta}$	λ robust stability	For MP = 2·0		
					λ_A	λ_B	λ_C
17	0·1	0·1	0·1	0·080	0·594	0·661	0·311
18	0·1	0·5	0·1	0·415	1·703	2·905	3·316
19	0·5	0·1	0·1	0·106	1·309	1·787	0·489
20	0·1	0·1	0·5	0·400	1·267	1·637	1·576
21	0·1	0·5	0·5	0·971	2·391	3·757	5.141
22	0·5	0·5	0·1	1·688	2·714	5·617	8·790
23	0·5	0·1	0·5	0·535	2·200	2·476	2·478
24	0·5	0·5	0·5	2·090	3·677	6·356	10·066

Table 3. Filter parameters resulting from tuning methods A–C. λ from robust stability condition is shown for comparison. In experiments 17–24 the ratio $\bar{\tau}/\bar{\theta} = 3·0$.

			Values for the filter parameter λ for these ratios of $\bar{\tau}/\bar{\theta}$						
$dk/\bar{k}$	$d\tau/\bar{\tau}$	$d\theta/\bar{\theta}$	0·05	0·1	0·5	1·0	3·0	10·0	30·0
0·0	0·0	0·0	0·000	0·000	0·000	0·000	0·000	0·000	0·000
0·0	0·1	0·0	0·030	0·062	0·196	0·245	0·277	0·283	0·285
0·1	0·0	0·0	0·265	0·266	0·266	0·265	0·265	0·265	0·266
0·0	0·0	0·1	0·192	0·192	0·196	0·192	0·192	0·192	0·192
0·0	0·1	0·1	0·199	0·203	0·268	0·339	0·399	0·415	0·418
0·1	0·1	0·0	0·267	0·271	0·360	0·417	0·457	0·468	0·469
0·1	0·0	0·1	0·400	0·400	0·400	0·400	0·400	0·400	0·400
0·1	0·1	0·1	0·403	0·410	0·454	0·525	0·594	0·612	0·617
0·1	0·5	0·1	0·433	0·447	0·758	1·109	1·703	2·041	2·157
0·5	0·1	0·1	1·097	1·102	1·115	1·199	1·309	1·342	1·349
0·1	0·1	0·5	1·100	1·106	1·104	1·136	1·267	1·338	1·355
0·1	0·5	0·5	1·130	1·155	1·189	1·412	2·391	3·102	2·318
0·5	0·5	0·1	1·128	1·161	1·293	1·833	2·714	3·226	3·395
0·5	0·1	0·5	1·977	1·987	1·998	2·012	2·200	2·292	2·319
0·5	0·5	0·5	2·020	2·059	2·125	2·312	3·677	4·666	5·017
0·0	0·0	0·0	0·000	0·000	0·000	0·000	0·000	0·000	0·000
0·1	0·1	0·1	0·403	0·410	0·454	0·525	0·594	0·612	0·617
0·2	0·2	0·2	0·777	0·784	0·799	0·959	1·179	1·267	1·292
0·3	0·3	0·3	1·166	1·185	1·166	1·403	1·860	2·099	2·164
0·4	0·4	0·4	1·573	1·607	1·621	1·855	2·674	3·189	3·349
0·5	0·5	0·5	2·020	2·059	2·125	2·312	3·667	4·666	5·017
0·6	0·6	0·6	2·485	2·538	2·664	2·765	4·884	6·724	7·498
0·7	0·7	0·7	2·974	3·053	3·215	3·216	6·341	9·819	11·478
0·8	0·8	0·8	3·499	3·595	3·837	3·659	8·152	14·892	18·926
0·9	0·9	0·9	4·051	4·166	4·479	4·280	10·192	24·200	37·169

Table 4. Controller parameters resulting from tuning method A. The ratio $\bar{\tau}/\bar{\theta}$ varies allowing the control system designer to interpolate between values for λ in the table to arrive at an acceptable tuning parameter.

Experiment	$dk/\bar{k}$	$d\tau/\bar{\tau}$	$d\theta/\bar{\theta}$	λ_A	λ_D	a	sup (15)	K	τ	θ
1	0·1	0·1	0·1	0·998	0·998	1·162	1·026	0·969	0·989	1·005
2	0·1	0·5	0·1	1·225	1·225	1·512	1·120	0·923	0·733	0·962
3	0·5	0·1	0·1	1·310	1·310	2·312	1·082	0·994	0·887	0·992
4	0·1	0·1	0·5	2·121	1·899	1·794	0·982	1·051	1·234	0·965
5	0·1	0·5	0·5	2·460	2·460	2·194	1·030	0·863	0·986	0·953
6	0·5	0·5	0·1	1·870	1·870	2·874	1·104	0·937	0·575	0·977
7	0·5	0·1	0·5	2·207	1·976	3·212	1·013	1·080	0·949	1·004
8	0·5	0·5	0·5	2·395	2·395	3·397	1·122	0·857	0·684	0·992

Table 5. Controller parameters resulting from optimization method D. The ratio $\bar{\tau}/\bar{\theta} = 1{\cdot}0$. Parameter a in the performance weight and λ from tuning method A are included for comparison. The structured singular value μ is shown for the system with the controller resulting from the optimization.

5.1. *Method A: tuning with actual uncertainty regions*

The first IMC filter-tuning method utilizes the loop transfer-function uncertainty regions $\pi(\omega)c(i\omega)$ to test for robust performance. Real parameter uncertainties in (1) are treated *exactly*. Once a filter parameter λ has been selected the sensitivity function with largest magnitude at each frequency given by

$$|s^*(\omega)| = \max_{p(i\omega)\in\Pi} \left| \frac{1}{1 + p(i\omega)c(i\omega)} \right| \tag{24}$$

is determined by locating the point closest to $(-1, 0)$ on each uncertainty region $\pi(\omega)c(i\omega)$. The filter parameter is adjusted until the robust performance requirement (14) has been satisfied. Increasing λ reduces the maximum peak in $|s^*(\omega)|$ and decreases the bandwidth of the system.

For the first-order with time-delay examples, the weight $w_2' = 1/MP = 1/2$ was used to specify performance requirements. Controller (23) was designed following the IMC procedure after selecting the nominal model (7). The IMC filter parameter λ was adjusted and regions $\pi(\omega)c(i\omega)$ located until the maximum peak in the sensitivity function $|s^*(\omega)|$ was determined to be 2. Values of λ leading to this result are listed in Tables 1–4. As expected, the filter parameter increases as the level of parameter uncertainty increases—less aggressive control action is required for robustness with respect to large modelling errors. The filter parameter increases slightly as a function of the ratio $\bar{\tau}/\bar{\theta}$.

5.2. *Method B: tuning with multiplicative error*

In the second IMC filter-tuning method the real parameter uncertainties in (1)–(3) are approximated by a multiplicative perturbation $l_m(i\omega)$ for the purposes of robustness analysis. The approximation is discussed in § 2.2 above. After the IMC controller has been designed and the filter form selected the IMC tuning parameters λ_i are implicitly defined by condition (15) for robust performance. If a performance weight $w_2' = 1/MP$ is selected filter parameters are adjusted iteratively until

$$\sup_{\omega} |\tilde{h}(i\omega)| l(\omega) + \frac{1}{MP} |(1 - \tilde{h}(i\omega))| = 1 \tag{25}$$

If the performance requirements are too severe it may not be possible to find values for the λ_i such that (15) is satisfied. When this situation is encountered it is possible that the less conservative tuning method based on the actual parameter uncertainties will lead to an acceptable design. If not, either the performance requirements must be relaxed or a different IMC filter form must be selected.

For the first-order with time-delay examples and performance weight $w_2' = 1/MP = 1/2$, condition (25) can be rewritten to yield an implicit expression for the filter paramater λ in controller (23):

$$\sup_{\omega} \frac{l(\omega)}{|\lambda i\omega + 1|} + \frac{1}{MP} \frac{|\lambda i\omega + 1 - \exp(-\bar{\theta} i\omega)|}{|\lambda i\omega + 1|} = 1 \tag{26}$$

Condition (26) represents the robust performance specification on the filter parameter λ. The robust stability requirement (11) is rewritten in terms of the filter parameter in (27) for comparison.

$$\sup_{\omega} \frac{l(\omega)}{|\lambda i\omega + 1|} < 1 \tag{27}$$

Values of λ leading to equality in (26) and (27) are listed in Tables 1–3 for each level of parameter uncertainty. Filter parameters required for robust performance are significantly larger than those required for robust stability in all of the examples. The same general trends are observed in the filter parameters for robust performance as in tuning method A. Note, however, that the values of λ from method B are slightly larger than those from method A. Conservativeness that entered the design procedure when parameter uncertainties were approximated by multiplicative uncertainty resulted in less aggressive control action.

5.3. *Method C: a quick design method*

At the frequency where the magnitude of the multiplicative uncertainty is equal to one condition (11) indicates that $\tilde{h}(i\omega)$ must already be rolled-off to prevent instability. This observation motivates a 'quick design' procedure for selecting the filter parameters λ_i. At the frequency ω' where $l(\omega') = 1$ the filter parameters can be implicitly defined by a conservative bound as follows:

$$|\tilde{h}(i\omega')|l(\omega') + |(1 - \tilde{h}(i\omega'))w_2(i\omega')| \leqslant |\tilde{h}(i\omega')|l(\omega') + (1 + |\tilde{h}(i\omega')|)w_2(i\omega')| = 1 \quad (28)$$

With $l(\omega') = 1$ and the choice of $w_2(i\omega') = 1/MP$ equation (28) becomes:

$$|\tilde{h}(i\omega')| = \frac{MP - 1}{MP + 1} \quad (29)$$

Equation (29) allows quick calculation of the IMC filter parameters λ_i once the frequency ω' at which $l(\omega') = 1$ has been located. Bound 1 enables quick calculation of ω' when simultaneous uncertainties in gain, time-constant, and time-delay are encountered. For example, see Fig. 4 where $\omega' = 9{\cdot}014\ \text{rad s}^{-1}$ for ten per cent uncertainty in k, τ and θ.

For the first-order with time-delay examples and the controller (23), at ω' the nominal complementary sensitivity function is given by $\tilde{h}(i\omega') = 1/(\lambda i\omega' + 1)$. Then equation (29) can be rewritten explicitly for λ as follows:

$$\lambda = \frac{\left[\left(\frac{MP + 1}{MP - 1}\right)^2 - 1\right]^{1/2}}{\omega'} \quad (30)$$

where MP is the desired maximum magnitude of the sensitivity function and ω' is the frequency at which $l(\omega') = 1$. Equation (30) with $MP = 2$ was used to calculate filter parameters shown in Tables 1–3. Although the filter parameters compare favourably with those obtained by the two methods discussed above the quick design method does *not* guarantee that the maximum peak in the sensitivity function will be less than MP. No such guarantee can be made since the quick design method considers only one frequency ω'. In fact, the filter parameters calculated using (30) for the examples with high levels of gain uncertainty lead to maximum peaks greater than 2. For those cases where gain uncertainty dominates (where the quick design method is least accurate) it is straightforward to tune the controller based on simple gain-margin arguments. Nevertheless, the data indicate that the quick design method will be useful for a wide range of uncertainty in model parameters. The filter parameter obtained via this method can certainly be used as a first guess for either of the more rigorous iterative methods A or B discussed above.

5.4. *Alternate nominal models*

The Smith predictor controller (21) resulting from the IMC design procedure contains more adjustable parameters than the λ_i in the IMC filter. All the parameters fixed by the choice of a nominal model also appear in the controller. Since the Smith predictor given by (20) with $\lambda = 0$ is known to be optimal for the processes (1)–(3) when there is no parameter uncertainty, the recommended IMC design method seems appropriately justified. Chen (1984), however, indicated that the nominal model with all parameters at their mean values does not always lead to an optimal control system design when the uncertainties are considered. Certainly it seems logical to fix nominal model parameters at their mean values when confronted by the process description (1)–(3). In order to evaluate the performance lost as a result of this selection another set of controller designs was performed for the first-order with time-delay examples in which all four controller parameters $\bar{k}$, $\bar{\tau}$, $\bar{\theta}$ and λ in (23) were optimized.

A control-relevant identification technique developed by Rivera and Morari (1986) was used to optimize all four parameters in the Smith predictor (23). Inputs to the optimization procedure include a nominal model, the magnitude of the multiplicative uncertainty, a performance weight w_2, and the structure of the model to be identified. The input nominal model was specified to be the centre of the smallest disk containing all models in the set (3). The optimization procedure selects a new nominal model and IMC filter parameter λ so as to reduce the structured singular value (15). Note that through the IMC design procedure selecting a new nominal model and filter parameter is tantamount to selecting new values for the parameters in the Smith predictor controller (11).

Table 5 lists the controller parameters selected by the optimization procedure for the same eight levels of uncertainty as in Table 1. The mean value for the three model parameters is 1·0 for all eight levels of uncertainty. In most cases the controller parameters in Table 5 do not differ significantly from 1·0. The weight w_2 in (18) with $b = 1/2$ and the parameter a indicated in Table 5 was input to the optimization procedure for each example. It can be verified using tuning method A that this is the best level of robust performance achievable with nominal model parameters at their mean values as in (7)—the system would fail the robust performance test (14) if parameter a had a value less than that indicated in Table 5. The optimization procedure attempted to reduce the supremum in (15) using a multiplicative error approximation for the actual parameter uncertainties. Values of the supremum for the eight designs are shown in Table 5. In the designs where the supremum is greater than one the additional conservativeness introduced by the multiplicative error approximation outweighted any benefit from optimizing all four parameters in the controller. These designs would not be considered robust based on the test involving the multiplicative error approximation. Results of this study indicate that selection of a nominal model with gain, time-constant, and time-delay at their mean values will, in most cases, lead to an acceptable Smith predictor controller.

5.5. *Structured-singular-value-optimal controller*

The structured-singular-value-optimal (SSV-optimal) controller is the controller that minimizes the supremum in (15). In this section the Smith predictor is compared with SSV-optimal controllers. The comparison illustrates how system performance might be effected by selecting the form of the controller to be that of the Smith predictor. The comparison also highlights differences in the SSV-optimal controllers

that result when process uncertainty is modelled with a single multiplicative uncertainty or with multiple real parameter uncertainties.

Both Smith predictor and SSV-optimal controllers were designed for the system modelled by (3). The nominal values of gain, time-constant and time-delay were all unity. The case of 50 per cent uncertainty in each of the three parameters was studied. Performance requirements were expressed in terms of the weight $w_2(i\omega)$ in (18) with $a = 3{\cdot}397$ and $b = 0{\cdot}5$. Recall that this level of robust performance was possible using a Smith predictor based on the nominal model and the tuning method in § 5.1 (see Table 5). The Smith predictor controller is given by (23) with $\lambda = 2{\cdot}395$.

The SSV-optimal controllers for the system were synthesized following the methods outlined in Chu *et al.* (1986) and Doyle (1982). Model uncertainty was represented by a single multiplicative uncertainty for synthesis of the first SSV-optimal controller. Figure 6 (*a*) shows the control structure with uncertainty and performance requirements written in terms of blocks Δ_1 and Δ_2 with norm $\|\Delta_i\|_2 \leqslant 1$. The structure 6 (*a*) can be rearranged into that shown in Fig. 7 (*a*). The SSV-optimal controller is then given by the stabilizing K which solves

$$\min_{D,K} \|DF_l(G; K)D^{-1}\|_\infty$$

where

$$F_l(G; K) = G_{11} + G_{12}K(I - G_{22}K)^{-1}G_{21}$$

and

$$D = \text{diag}\,(d_1, d_2, \ldots, d_n)$$

with n being the number of blocks in

$$\Delta = \text{diag}\,(\Delta_1, \Delta_2, \ldots, \Delta_0)$$

The HONEYX† computer software used to synthesize the SSV-optimal controller requires rational approximations of all irrational transfer functions appearing in the block structure. Hence, a fourth-order Padé approximation was substituted for the time-delay in $\tilde{p}$; a first-order Padé approximation, for the time-delay in the bound (8) for L_m (see the dashed curve in Fig. 2).

For synthesis of the second SSV-optimal controller model uncertainty was represented by individual parameter uncertainties. Figure 6 (*b*) shows individual uncertainties in gain, time-constant and time-delay written in terms of three blocks Δ_1, Δ_2 and Δ_3. Note that the block structure represents a first-order Padé approximation for the time-delay. Figure 7 (*b*) illustrates the equivalent interconnection structure for that in Fig. 6 (*b*). The HONEYX software assumes each Δ_i is a complex perturbation with $\|\Delta_i\|_2 \leqslant 1$ even though they represent real parameter variations.

The magnitude and phase of the two SSV-optimal controllers are shown in Fig. 8. The controller resulting when a single multiplicative uncertainty was used (labelled 2 in Fig. 8) was 18th order. The controller resulting when multiple parameter uncertainties were used (labelled 3 in Fig. 8) was 19th order. Note in Fig. 8 that both SSV-optimal controllers have slightly lower gain than the Smith predictor (labelled 1) for frequencies below one. The magnitude of model uncertainty is low over this

† Developed by Honeywell Systems and Research Center, Minneapolis, Minnesota, U.S.A.

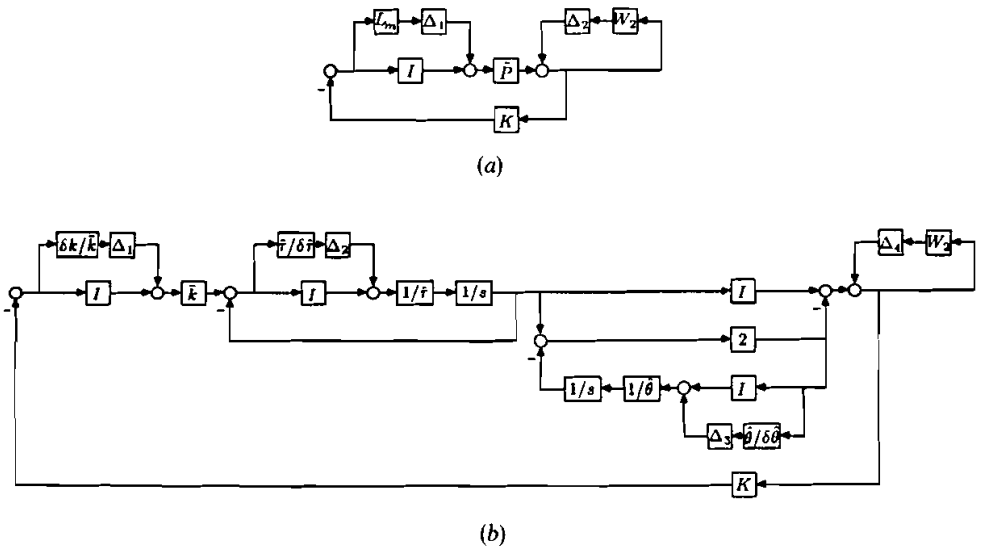

Figure 6. Feedback control structures incorporating a single multiplicative uncertainty (*a*) and individual gain, time-constant and time-delay uncertainty (*b*) are shown. In (*b*) a first-order Padé approximation is used to represent time-delay. Since the inverse of τ and θ appear in (*b*) the following variables are used to define real parameter variations: $1/\tilde{\tau} = (1/2\tau_{\min}) + (1/2\tau_{\max})$, $1/\hat{\theta} = (1/2\theta_{\min}) + (1/2\theta_{\max})$, $1/\delta\tilde{\tau} = (1/\tilde{\tau}) - (1/\tau_{\max})$, $1/\delta\hat{\theta} = (1/\hat{\theta}) - (1/\theta_{\max})$.

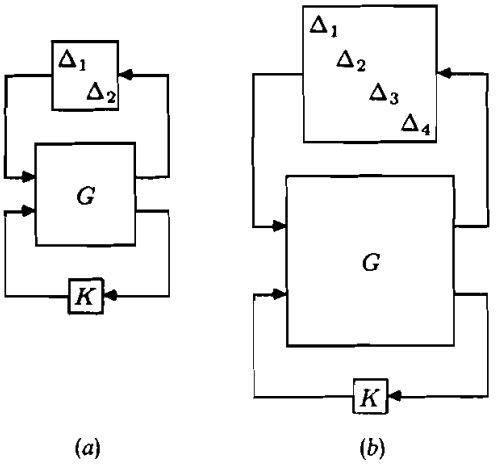

Figure 7. The two feedback structures in Fig. 7 can be rewritten as shown with interconnection matrix G, norm-bounded matrix Δ and controller K.

frequency range; hence the controller shape is largely determined by the performance weight w_2. At higher frequencies the SSV-optimal controllers employ higher gain than the Smith predictor. The higher gain causes oscillation in the nominal sensitivity function in the high frequency range as shown in Fig. 9. The SSV-optimal controllers reduce the structured singular value (see Fig. 10) at frequencies near 0·3 where the performance requirement is tight and increase it at higher frequencies where the performance requirement allows additional gain. Note that there is little difference

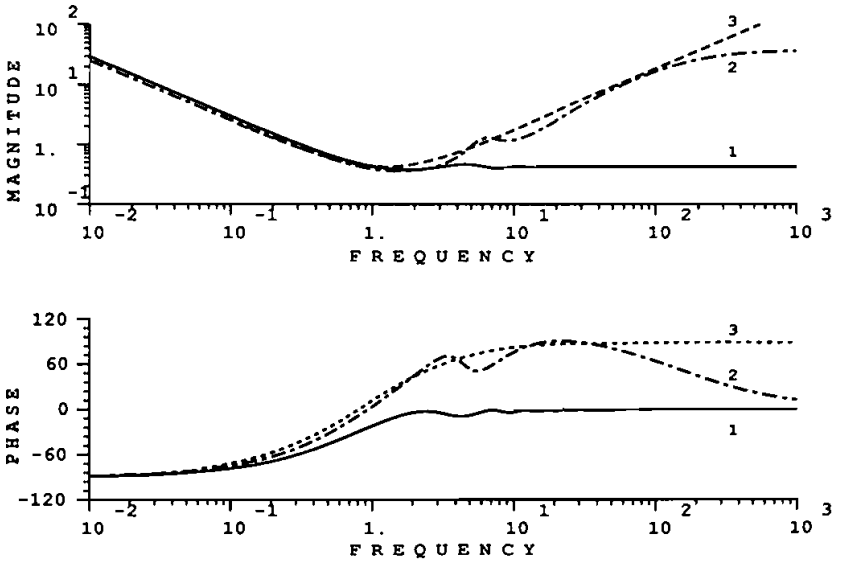

Figure 8. The Bode plots of SSV-optimal and Smith predictor controllers are quite similar in the low frequency range. Curve 1 is the Smith predictor. The SSV-optimal controllers synthesized using multiplicative uncertainty and parameter uncertainty are curves 2 and 3, respectively.

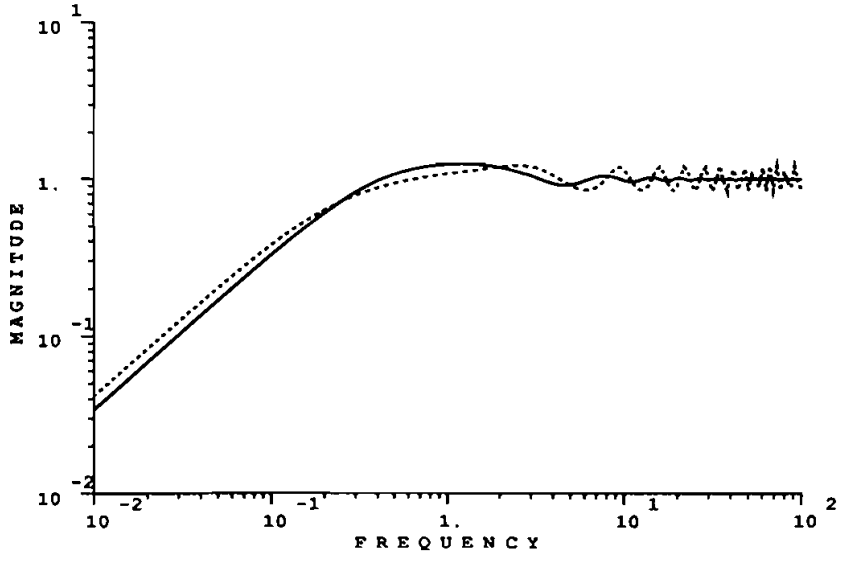

Figure 9. The sensitivity function for the system with SSV-optimal controller (dashed curve) has larger amplitude oscillations in the high frequency range than does that with the Smith predictor controller (solid line). The sensitivity functions with the two SSV-optimal controllers are indistinguishable from one another.

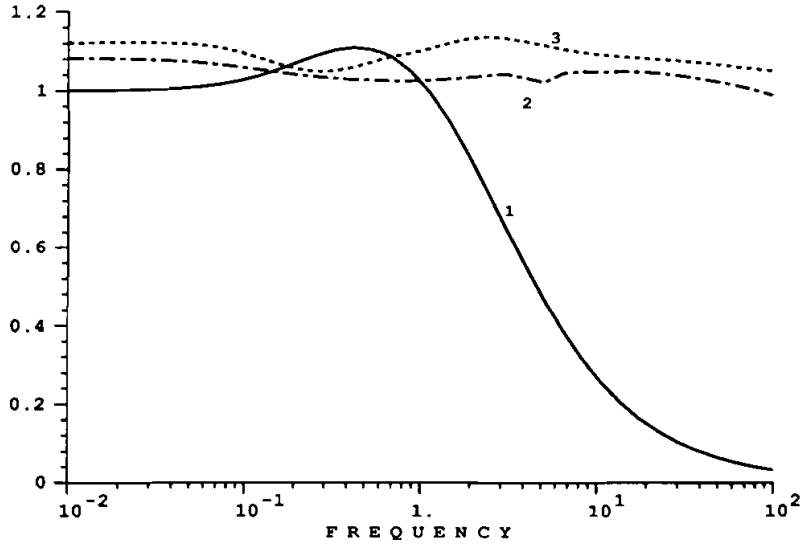

Figure 10. The structured singular values for the control system with SSV-optimal controllers (2 and 3) and Smith predictor controller (1) are compared here. Structured singular values with SSV-optimal controllers synthesized using multiplicative uncertainty and parameter uncertainty are on curves 2 and 3, respectively.

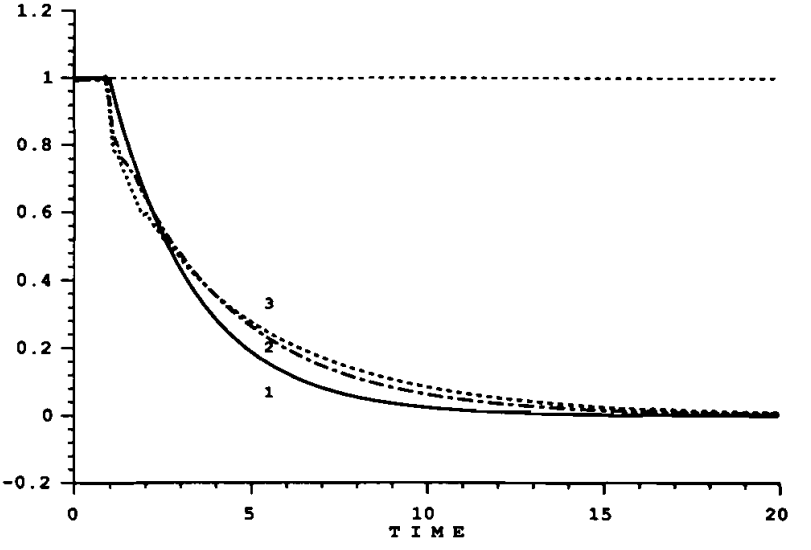

Figure 11. Responses to step disturbances are quite similar for the system with Smith predictor (1), with SSV-optimal controller synthesized using multiplicative uncertainty (2), and with the SSV-optimal controller synthesized using parameter uncertainties (3).

between the two SSV-optimal controllers in Figs. 8 and 10, indicating that relatively little conservativeness entered the design when the Δ_i representing real parameters were assumed to be complex. This outcome may be limited to this example, however, since such an assumption can in general be quite conservative. All structured singular values in Fig. 10 are greater than one, indicating that the performance requirement w_2 would have to be relaxed in order for the system to pass the robust performance test based on the norm-bounded blocks Δ_i. Recall that the robust performance test based on the actual uncertainty regions can be passed using the same requirement w_2 used in Fig. 10.

Figure 11 shows the nominal system response to step disturbances with Smith predictor and SSV-optimal controllers. There is relatively little difference in nominal system response despite the complexity of the SSV-optimal controllers.

6. Discussion and conclusions

The internal model control structure provides a useful framework for the design and tuning of robust Smith predictor controllers for systems with time-delay. Results of this study offer several alternatives to the control system designer confronted with the task of designing robust controllers for processes modelled by transfer-functions with real-parameter uncertainties. An H_2-optimal IMC controller can easily be designed for the nominal model and expected disturbance using the results of § 4. Augmenting the controller with a filter can ensure robust performance despite parameter uncertainties. The IMC filter can be tuned following the methods outlined in § 5 or the model can be non-dimensionalized (see § 6.1) allowing the use of tabulated filter-tuning constants. The Smith predictor that results from the IMC design procedure compares favourably with the SSV-optimal controller for systems with time-delay. Simultaneous parameter uncertainties can be considered exactly when testing for robust performance, or they can be approximated by a single multiplicative uncertainty for mathematical convenience. Bound 1 in § 2.2 gives an exact expression for the magnitude of multiplicative uncertainty that can be used to approximate simultaneous uncertainties in gain, time-constant and time-delay. Use of Bound 1 in SSV-optimal controller synthesis was demonstrated.

6.1. *Non-dimensionalizing the model*

When confronted with a stable process described by (6) the control designer can non-dimensionalize the model enabling use of tuning parameter data in Table 4. Model (6) with $p'(s) = 1$ can be rewritten as follows:

$$p^*(s^*) = \frac{p(s)}{k} = \frac{(1+\delta k^*)\exp(-(1+\delta\theta^*)s^*)}{(1+\delta\tau^*)\frac{\bar{\tau}}{\bar{\theta}}s^* + 1}$$

where dimensionless parameters are defined by

$$s^* = s\bar{\theta}, \quad dk^* = \frac{\delta k}{\bar{k}}, \quad \delta\tau^* = \frac{\delta\tau}{\bar{\tau}}, \quad \delta\theta^* = \frac{\delta\theta}{\bar{\theta}}$$

Note that the following bounds are implied for the dimensionless parameters:

$$|\delta k^*| < 1, \quad |\delta\tau^*| < 1, \quad |\delta\theta^*| < 1, \quad 0 < \frac{\bar{\tau}}{\bar{\theta}} < \infty$$

A dimensionless IMC controller $q^*(s^*)$ can be designed for $p^*(s^*)$ with the appropriate filter parameter λ^* found by interpolating between values listed in Tables 1–4.

The real controller $q(s)$ is related to its dimensionless counterpart as follows:

$$q(s) = \frac{q^*(s\bar{\theta})}{\bar{k}}$$

The real controller $q(s)$ will have an IMC filter parameter given by

$$\lambda = \lambda^* \bar{\theta}$$

6.2. *Simulating the worst case response*

The time-domain behaviour of the system can be investigated by simulating the response of the 'worst case' sensitivity function to selected disturbances. When the regions $\pi(\omega)c(i\omega)$ are located the closest point on each region to $(-1, 0)$ defines the sensitivity function $s^*(\omega)$ as in (24). The magnitude of $s^*(\omega)$ at each frequency will be greater than or equal to the magnitude of any sensitivity function resulting from a model in (4). The response of $s^*(\omega)$ to different types of disturbances can be determined by inverse Fourier transform. If the process model is accurate, the integral square error in the response of the real system to each of these disturbances will be less than that in the response of $s^*(\omega)$ to the same disturbance. The shape of the response of $s^*(\omega)$, however, may not resemble the real system response since different models in Π contribute to $s^*(\omega)$ at different frequencies. Nevertheless, $s^*(\omega)$ can provide a useful measure of the system's disturbance rejection capability.

Responses of $s^*(\omega)$ to step disturbances are shown in Fig. 12 for 10 per cent and 50 per cent uncertainty in each of the three parameters k, τ and θ in the first-order with

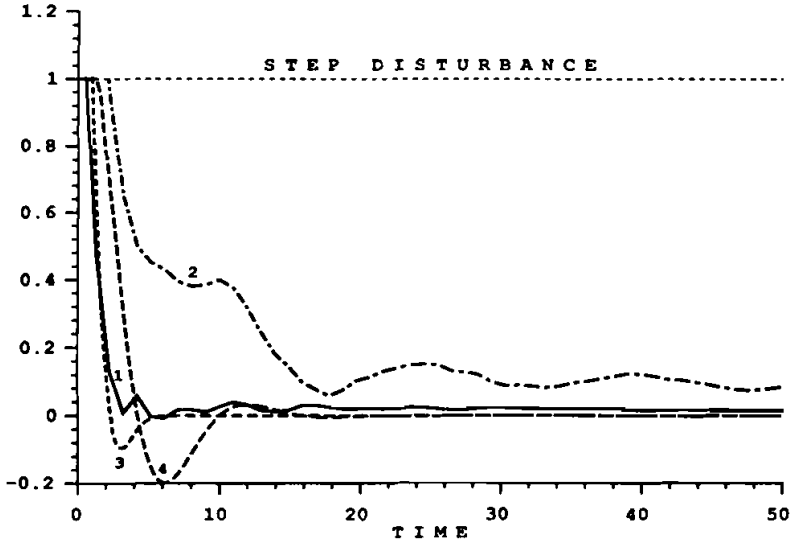

Figure 12. Using the Smith predictors resulting from tuning method A, the responses of $s^*(\omega)$ to step disturbances are shown for 10 per cent parameter uncertainty (curve 1) and 50 per cent parameter uncertainty (curve 2) in model (6). Responses of the model $p(s) = k \exp(-\theta s)/(\tau s + 1)$ with $k = \bar{k} + \Delta k$, $\tau = \bar{\tau} + \Delta\tau$ and $\theta = \bar{\theta} + \Delta\theta$ are shown using the same controllers for 10 per cent parameter uncertainty (curve 3) and 50 per cent parameter uncertainty (curve 4).

time-delay model. The worst case integral-square-error $\|e(t)\|_2^2$ for these two examples was calculated to be 2·258 and 6·425, respectively. A real system response to the step disturbance is shown for comparison at each of the two levels of uncertainty. The three parameters were specified to be at their highest values in the model used for the real system response: $k = \bar{k} + \Delta k$, $\tau = \bar{\tau} + \Delta\tau$ and $\theta = \bar{\theta} + \Delta\theta$. For 10 per cent parameter uncertainty and 50 per cent parameter the integral-square-error in the response of the real system to the step disturbance was calculated to be 1·304 and 2·335 for 10 per cent parameter uncertainty and 50 per cent parameter uncertainty, respectively. The integral-square-error in the response of the real first-order with time-delay system is less than that of $s^*(\omega)$. This is to be expected since $s^*(\omega)$ is the worst combination of parameter values at each frequency (an ∞-norm bound on the magnitude of the sensitivity function) rather than one particular first-order with time-delay model. The extent to which $s^*(\omega)$ gives a conservative estimate of the two-norm of the error emphasizes the inherent conservativeness introduced when transfer functions with real parameter uncertainties are represented by uncertainty regions on the complex plane—the parametric structure of the process model is lost. It also emphasizes the lack of clarity in the relationship between ∞-norm performance requirements and the eventual time-domain behaviour of the system.

6.3. *Additional applications*

Bound 1 and Bound 2 (see the Appendix) provide particularly useful links between parameter uncertainties and multiplicative error for simple process models. The bounds can be applied to higher order models if uncertainty can be accurately represented by variations in three parameters: gain, time-delay and one pole location or gain, time-delay and one zero location. In MIMO systems where low-order dynamics $g_{ii}(s)$ with parameter uncertainties can be factored out along the diagonal of the matrix transfer-function as shown below, the bounds can be applied to approximate the parameter uncertainties by multiplicative perturbations.

$$\begin{bmatrix} p_{11}(s) & p_{12}(s) \\ p_{21}(s) & p_{22}(s) \end{bmatrix} = \begin{bmatrix} \tilde{f}_{11}(s) & \tilde{f}_{12}(s) \\ \tilde{f}_{21}(s) & \tilde{f}_{22}(s) \end{bmatrix} \begin{bmatrix} g_{11}(s) & 0 \\ 0 & g_{22}(s) \end{bmatrix}$$

$$= \begin{bmatrix} \tilde{f}_{11}(s) & \tilde{f}_{12}(s) \\ \tilde{f}_{21}(s) & \tilde{f}_{22}(s) \end{bmatrix} \begin{bmatrix} \tilde{g}_{11}(s) & 0 \\ 0 & \tilde{g}_{22}(s) \end{bmatrix} \left(\begin{bmatrix} 1 & 0 \\ 0 & 1 \end{bmatrix} + \begin{bmatrix} l_{m_{11}}(s) & 0 \\ 0 & l_{m_{22}}(s) \end{bmatrix} \right)$$

Certain types of actuator uncertainty and input uncertainty are accurately described in this manner (see Skogestad and Morari 1986 for a distillation column example). Representing MIMO modelling error with different multiplicative uncertainties in each input direction can be less conservative than representing it with a single multiplicative perturbation to the whole matrix transfer-function. Approximating the parameter uncertainties in the MIMO transfer-function matrix with multiplicative uncertainties $l_{m_{11}}(s)$ and $l_{m_{22}}(s)$ also allows convenient application of structured singular value analysis for robust performance.

Appendix

Definition of variables

The description (6) for a set of process models can be rewritten as follows:

$$p(s) = p'(s)\frac{(\bar{k}+\delta k)}{(\bar{\tau}+\delta\tau)s+1}\exp\left[-(\bar{\theta}+\delta\theta)s\right]$$

$$p(s) = p'(s)\frac{\bar{k}}{\bar{\tau}s+1}\exp(-\bar{\theta}s)\left[1+\left(\frac{\bar{k}+\delta k}{\bar{k}}\right)\left(\frac{\bar{\tau}s+1}{(\bar{\tau}+\delta\tau)s+1}\right)\exp(-\delta\theta s)-1\right] \quad \text{(A 1)}$$

$$p(s) = \tilde{p}(s)[1+l_m(s)] \quad \text{(A 2)}$$

From equations (A 1) and (A 2) we can identify expressions for $\tilde{p}(s)$ and $l_m(s)$.

$$\tilde{p}(s) = \frac{\bar{k}}{\bar{\tau}s+1}\exp(-\bar{\theta}s) \quad \text{(A 3)}$$

$$l_m(s) = \left(\frac{\bar{k}+\delta k}{\bar{k}}\right)\left(\frac{\bar{\tau}s+1}{(\bar{\tau}+\delta\tau)s+1}\right)\exp(-\delta\theta s)-1 \quad \text{(A 4)}$$

Bound 1 gives the smallest bound $l(\omega)$ such that $|l_m(i\omega)| \leqslant l(\omega)$ for all δk, $\delta\tau$ and $\delta\theta$. The proof will be approached from the perspective of determining the greatest distance of $l_m(s)+1$ from the point (1, 0). Clearly this distance will be the bound $l(\omega)$. With $|\delta k| \leqslant \Delta k$, $|\delta\tau| \leqslant \Delta\tau$ and $|\delta\theta| \leqslant \Delta\theta$ all possible values for $l_m(s)+1$ at one frequency $s = i\omega$ can be located inside the boundary $ABCDEF$ sketched in Fig. 13 (Laughlin *et al.* 1986). Along curve AB $\delta k = \Delta k$, $\delta\tau = -\Delta\tau$ and $\delta\theta$ varies. Along curve BC $\delta k = \Delta k$, $\delta\theta = -\Delta\theta$ and $\delta\tau$ varies. Along curve CD $\delta\tau = \Delta\tau$, $\delta\theta = -\Delta\theta$ and δk varies. Along curve DE $\delta k = -\Delta k$, $\delta\tau = \Delta\tau$ and $\delta\theta$ varies. Along curve EF, $\delta k = -\Delta k$, $\delta\theta = \Delta\theta$ and $\delta\tau$ varies. Along curve FA, $\delta\tau = -\Delta\tau$, $\delta\theta = \Delta\theta$ and δk varies. Equation (10) specifies the frequency ω^* when $\arg[A] = \pi$. Bound 1 claims that point A on Fig. 13 is farther from (1, 0) than any other point on the boundary of the region $ABCDEF$ for frequencies less than ω^*. Proving this claim is possible by considering the individual contributions of gain, time-constant and time-delay uncertainty to $l_m(s)+1$.

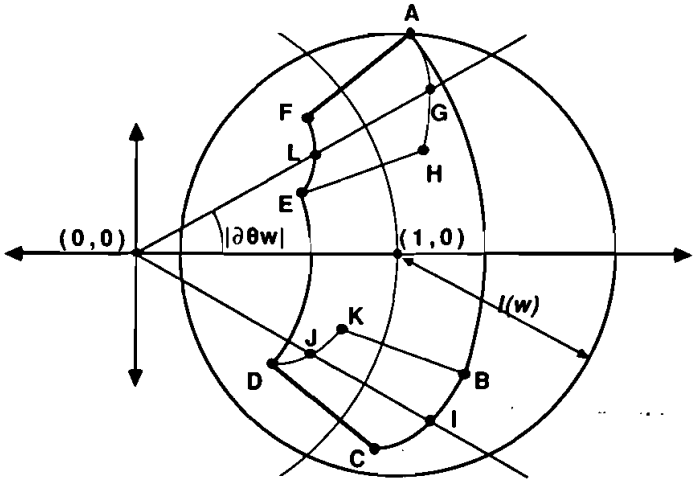

Figure 13. All possible values for $l_m(s)+1$ at one frequency $s = i\omega$ can be located inside the boundary $ABCDEF$ given the parameter uncertainties in (6). The bound $l(\omega)$ on the magnitude of the multiplicative uncertainty is equal to the radius of the smallest disk centred at (1, 0) that contains the region boundary.

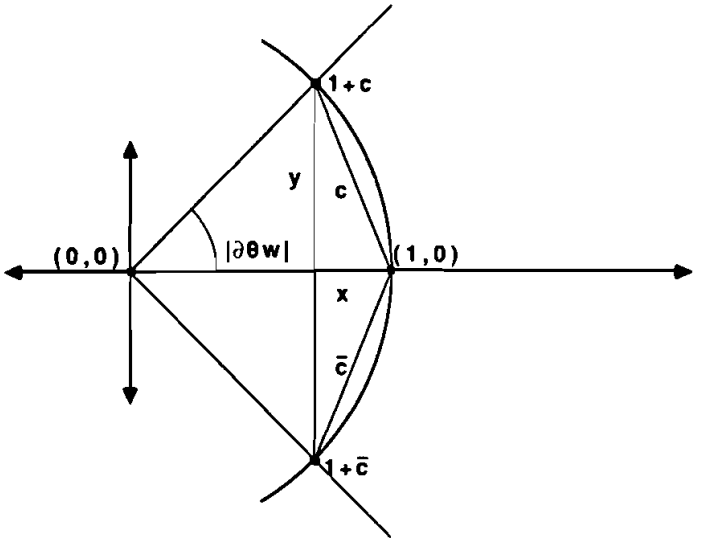

Figure 14. The contribution of time-delay uncertainty to $l_m(s)+1$.

Figure 14 represents the contribution of time-delay uncertainty to $l_m(s)+1$; that is, $\exp(+|\delta\theta|s) = 1+c$ and $\exp(-|\delta\theta|s) = 1+\bar{c}$. Restrict $|\delta\theta|\omega \leqslant \pi$ to define positive $x = 1-\cos(|\delta\theta|\omega)$ and positive $y = \sin(|\delta\theta|\omega)$. Then $c = -x+iy$ and it is easily verified that

$$-2x + x^2 + y^2 = 0 \tag{A 5}$$

The contribution of gain uncertainty to $l_m(s)+1$ is $(\bar{k}+|\delta k|)/\bar{k} = 1+r$ and $(\bar{k}-|\delta k|)/\bar{k} = 1-r$ where positive $r = |\delta k|/\bar{k}$.

Figure 15 represents the contribution of a left-half plane pole uncertainty to $l_m(s)+1$; that is $(\bar{\tau}s+1)/((\bar{\tau}-|\delta\tau|)s+1) = 1+b$ and $(\bar{\tau}s+1)/((\bar{\tau}+|\delta\tau|)s+1) = 1+d$

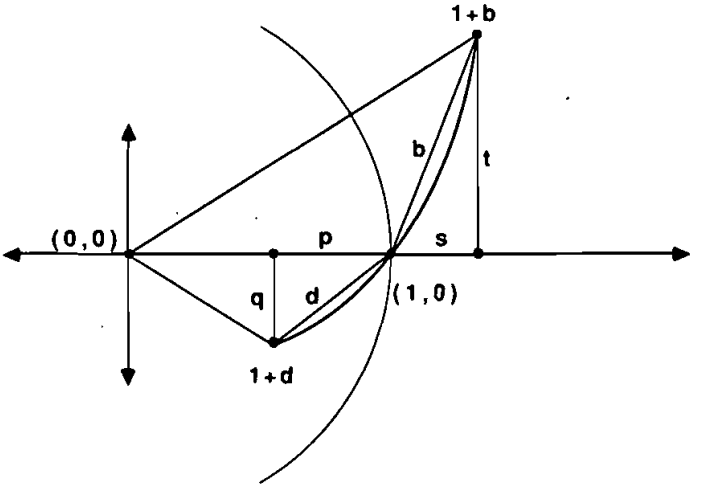

Figure 15. The contribution of left-half-plane pole uncertainty to $l_m(s)+1$.

where $b = s + it$, $d = -p - iq$, and positive s, t, p and q are defined below.

$$s = \frac{|\delta\tau|(\bar{\tau} - |\delta\tau|)\omega^2}{1 + (\bar{\tau} - |\delta\tau|)^2\omega^2}$$

$$t = \frac{|\delta\tau|\omega}{1 + (\bar{\tau} - |\delta\tau|)^2\omega^2}$$

$$p = \frac{|\delta\tau|(\bar{\tau} + |\delta\tau|)\omega^2}{1 + (\bar{\tau} + |\delta\tau|)^2\omega^2}$$

$$q = \frac{|\delta\tau|\omega}{1 + (\bar{\tau} + |\delta\tau|)^2\omega^2}$$

Since $|b| \geqslant |d|$ for all values of ω, $\bar{\tau} > 0$, and $|\delta\tau| \leqslant \bar{\tau}$ the following inequalities are easily verified:

$$s^2 + t^2 - p^2 - q^2 \geqslant 0 \tag{A 6}$$

$$t - q \geqslant 0 \tag{A 7}$$

$$s^2 + t^2 + p^2 + q^2 + s - p = |\delta\tau|\bar{\tau}\left(\frac{1}{1 + (\bar{\tau} - |\delta\tau|)^2\omega^2} - \frac{1}{1 + (\bar{\tau} + |\delta\tau|)^2\omega^2}\right) \geqslant 0 \tag{A 8}$$

The following lemmas will be used in the proof of Bound 1. For brevity they are presented here without proof. The reader can easily establish their validity via simple geometrical arguments.

Lemma 1

Consider a circle centered at the origin. Let XY be an arc of the circle passing through the positive real axis having endpoints X and Y. If $|\arg[X]| \leqslant \pi$ and $|\arg[Y]| \leqslant \pi$ then the point on XY with maximum distance from $(1, 0)$ is X if $|\arg[X]| > |\arg[Y]|$ or Y if $|\arg[Y]| > |\arg[X]|$.

Lemma 2

Consider a ray originating from $(0, 0)$. Let XYZ be a line segment on the ray with midpoint Y on or outside the unit circle and endpoint X nearest the origin. The point on XYZ with maximum distance from $(1, 0)$ is endpoint Z farthest from the origin.

Lemma 3

Consider a ray originating from $(0, 0)$. Let XYZ be a line segment on the ray with midpoint Y inside the unit circle and endpoint X nearest the origin. The point on XYZ with maximum distance from $(1, 0)$ is either endpoint X or endpoint Z.

Proof of Bound 1

Consider Fig. 13 illustrating the region containing possible values for $l_m(i\omega) + 1$ when $\bar{\tau} > 0$. The following arguments prove that of all points on boundary $ABCDEF$, point A is at the maximum distance from $(1, 0)$ at frequencies below ω^*.

(i) $|A - 1|$ is greater than or equal to the distance from $(1, 0)$ to any point on arc AB (Lemma 1).

(ii) $|A-1|$ is greater than or equal to the distance from $(1,0)$ to any point on segment FA (Lemma 2).

(iii) The distance from $(1,0)$ to any point on BI is less than or equal to the distance from $(1,0)$ to a corresponding point on AG (Lemma 1).

(iv) The distance from $(1,0)$ to any point on FL is less than or equal to the distance from $(1,0)$ to a corresponding point on AG (Lemma 2).

(v) The distance from $(1,0)$ to any point on EL is less than or equal to the distance from $(1,0)$ to a corresponding point on DJ (Lemma 1).

(vi) $|E-1|$ is greater than or equal to the distance from $(1,0)$ to any point on arc DE (Lemma 1).

(vii) $|A-1|$ is greater than the distance from $(1,0)$ to any other point on AG because AG lies outside the unit circle and both magnitude and argument of A are greater than those of any other point on AG.

(viii) Either $|C-1|$ or $|D-1|$ is greater than or equal to the distance from $(1,0)$ to any other point on CD (Lemma 3).

(ix) $|A-1| \geqslant |C-1|$ since

$$\begin{aligned}|A-1|^2-|C-1|^2 &= (1+2r+r^2)(s^2+t^2-p^2-q^2)\\ &\quad +2y(1+r)(t-q)\\ &\quad +2x(1+r)(p+s)+2r(s+p)+2pr^2 \geqslant 0\end{aligned}$$

(Equations (A 5)–(A 8) with r, s, t, p, q, x and y all positive.)

(x) $|A-1| \geqslant |D-1|$ since

$$\begin{aligned}|A-1|^2-|D-1|^2 &= (1+r^2)(s^2+t^2-p^2-q^2)\\ &\quad +2r(s^2+t^2+p^2+q^2+s-p)\\ &\quad +2px(1-r)+2y(t-q)+2ry(t+q)+2sx(1+r)\\ &\quad +2pr^2+4rx+2r^2s \geqslant 0\end{aligned}$$

(Equations (A 5)–(A 8) with r, s, t, p, x, and y all positive.)

(xi) Points on DJ and CI are not farther from $(1,0)$ than point A because arguments (vii)–(x) can be applied with smaller $\delta\tau$.

Therefore $l(\omega) = |A-1|$ for $\omega \leqslant \omega^*$.

For $\omega > \omega^*$ Bound 1 follows from the triangle inequality and the fact that the model described by the extremes of gain, time-constant, and time-delay in Bound 1 is a member of the set described by (6).

The region containing all possible values for $l_m(i\omega)+1$ when $\bar{\tau} < 0$ is the mirror image of that in Fig. 13 across the real axis. The same arguments apply for the proof in this case with $s = -i\omega$, hence the change of signs in Bound 1 when $\bar{\tau} < 0$. □

The proof of Bound 1 motivates a similar bound on the magnitude of the multiplicative error when simultaneous parameter uncertainties in process gain, zero location and time-delay are encountered.

Bound 2: gain, time-delay and zero uncertainty

Consider the following set of process models:

$$p(s) = p'(s)(\bar{k}+\delta k)((\bar{z}+\delta z)s+1)\exp\left[-(\bar{\theta}+\delta\theta)s\right] \qquad \text{(A 9)}$$

where $p'(s)$ does not contain parameter uncertainties and $\bar{k}$, $\bar{z}$, $\bar{\theta}$, δk, δz and $\delta\theta$ are defined by:

$$\bar{k} = \frac{k_{\min} + k_{\max}}{2}, \quad \bar{z} = \frac{z_{\min} + z_{\max}}{2}, \quad \bar{\theta} = \frac{\theta_{\min} + \theta_{\max}}{2}$$

$$|\delta k| \leqslant \Delta k = |k_{\max} - \bar{k}| < |\bar{k}|, \quad |\delta z| \leqslant \Delta z = |z_{\max} - \bar{z}| < |\bar{z}|$$

$$|\delta\theta| \leqslant \Delta\theta = |\theta_{\max} - \bar{\theta}| < |\bar{\theta}|$$

Define a nominal model $\tilde{p}(s)$ with gain, zero and time-delay at their mean values:

$$\tilde{p}(s) = p'(s)\bar{k}(\bar{z}s + 1)\exp(-\bar{\theta}s) \tag{A 10}$$

The smallest possible bound $l(\omega)$ on the multiplicative error $l_m(s)$ such that all models in (A 9) are contained in the set $p(s) = \tilde{p}(s)[1 + l_m(s)]$ is given by:

$$l(\omega) = \left|\left(\frac{|\bar{k}| + \Delta k}{|\bar{k}|}\right)\left(\frac{(\bar{z} \pm \Delta z)i\omega + 1}{\bar{z}i\omega + 1}\right)\exp(\pm\Delta\theta i\omega) - 1\right|, \quad \forall\,\omega < \omega^{**} \tag{A 11}$$

$$l(\omega) = \left|\left(\frac{|\bar{k}| + \Delta k}{|\bar{k}|}\right)\left(\frac{(\bar{z} \pm \Delta z)i\omega + 1}{\bar{z}i\omega + 1}\right)\right| + 1, \quad \forall\,\omega \geqslant \omega^{**} \tag{A 12}$$

where ω^{**} is defined implicitly by:

$$\pm\Delta\theta\omega^{**} + \arctan\left[\frac{\pm\Delta z\omega^{**}}{1 + \bar{z}(\bar{z} \pm \Delta z)\omega^{**2}}\right] = \pm\pi, \quad \frac{\pi}{2} \leqslant \Delta\theta\omega^{**} \leqslant \pi \tag{A 13}$$

Bound 2 applies to both left- and right-half-plane zeros in (A 3). Top signs are selected in (A 11)–(A 13) if $\bar{z}$ is positive, indicating a left-half-plane zero. Bottom signs are selected in (A 11)–(A 13) if $\bar{z}$ is negative, indicating a right-half-plane zero.

The similarity between Bound 1 for simultaneous uncertainties in gain, pole location and time-delay and Bound 2 for simultaneous uncertainties in gain, zero location and time-delay can be seen by examining $l_m(s)$. The description (A 9) for a set of process models can be rewritten as follows:

$$p(s) = p'(s)(\bar{k} + \delta k)((\bar{z} + \delta z)s + 1)\exp[-(\bar{\theta} + \delta\theta)s]$$

$$p(s) = p'(s)\bar{k}(\bar{z}s + 1)\exp(-\bar{\theta}s)\left[1 + \left(\frac{\bar{k} + \delta k}{\bar{k}}\right)\left(\frac{(\bar{z} + \delta z)s + 1}{\bar{z}s + 1}\right)\exp(-\delta\theta s) - 1\right] \tag{A 14}$$

$$p(s) = \tilde{p}(s)[1 + l_m(s)] \tag{A 15}$$

From equations (A 14) and (A 15) we can identify (A 10) as the expression for the nominal model $\tilde{p}(s)$ and the following expression as $l_m(s)$:

$$l_m(s) = \left(\frac{\bar{k} + \delta k}{\bar{k}}\right)\left(\frac{(\bar{z} + \delta z)s + 1}{\bar{z}s + 1}\right)\exp(-\delta\theta s) - 1 \tag{A 16}$$

Figure 16 represents the contribution of a left-half plane zero uncertainty to $l_m(s) + 1$; that is, $((\bar{z} + |\delta z|)s + 1)/(\bar{z}s + 1) = 1 + a$ and $((\bar{z} - |\delta z|)s + 1)/((\bar{z}s + 1) = 1 - a$ where $a = u + iv$ with positive u and v defined below.

$$u = \frac{|\delta z|\bar{z}\omega^2}{1 + \bar{z}^2\omega^2}$$

$$v = \frac{|\delta z|\omega}{1 + \bar{z}^2\omega^2}$$

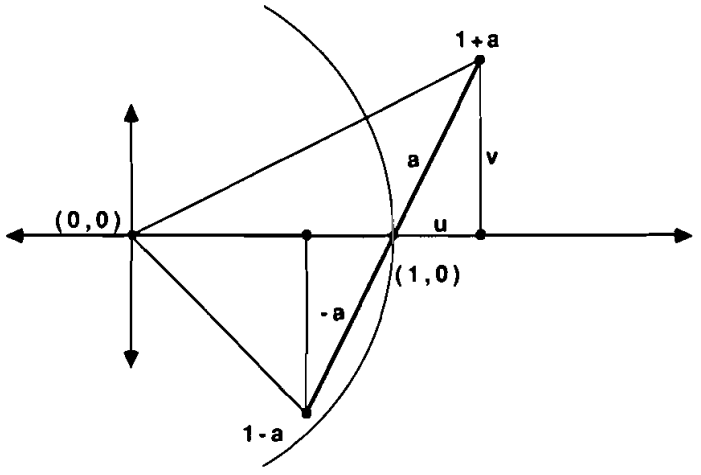

Figure 16. The contribution of left-half-plane zero uncertainty to $l_m(s)+1$.

Proof of Bound 2 uses the same arguments used to prove Bound 1. The only modification required is that the zero uncertainty replace the pole uncertainty by setting $s=p=u$ and $t=q=v$ in the proof for the case $\bar{z}<0$. Subsequently set $s=-i\omega$ in the proof for the case $\bar{z}>0$. The substitution $s=-i\omega$ necessitates the change of signs in (6)–(8) for the case $\bar{z}>0$.

References

Åström, K. J., 1977, *Int. J. Control*, **26**, 307.

Bhaya, A., and Desoer, C. A., 1985, *Int. J. Control*, **41**, 813.

Brosilow, C. B., 1979, The structure and design of Smith predictors from the viewpoint of inferential control. *Joint American Control Conf.*, Denver.

Callender, A., Hartree, D. R., and Porter, A., 1936, *Phil. Trans. R. Soc.*, **235**, 415.

Chen, S., 1984, Control system design for multivariable uncertain processes. Ph.D. thesis, Case Western Reserve University.

Chu, C. C., Doyle, J. C., and Lee, E. B., 1986, *Int. J. Control*, **44**, 565.

Cohen, G. H., and Coon, G. A., 1953, *Trans. Am. Soc. mech. Engrs*, July, 827.

Doyle, J. C., 1982, *Proc. Instn elect. Engrs*, Pt D, **129**, 242.

East, D. J., 1981, *Int. J. Control*, **34**, 731; 1982, *Ibid.*, **35**, 891.

Garcia, C. E., and Morari, M., 1982, *I. & E.C. Process Des. Dev.*, **21**, 308.

Holt, B. R., 1984, The assessment of dynamic resilience: the effect of non-minimum phase elements. Ph.D. thesis, University of Wisconsin–Madison.

Horowitz, I., 1983, *Int. J. Control*, **38**, 977.

Ioannides, A. C., Rogers, G. J., and Latham, V., 1979, *Int. J. Control*, **29**, 557.

Jerome, N. F., and Ray, W. H., 1986, *A.I.Ch.E. Jl*, **32**, 914.

Laughlin, D. L., Jordan, K. G., and Morari, M., 1986, *Int. J. Control*, **44**, 1675.

Morari, M., Zafirou, E., and Economou, C., 1987, *Robust Process Control* (Berlin: Springer-Verlag).

Ogunnaike, B. A., Lemaire, J. P., Morari, M., and Ray, W. H., 1983, *A.I.Ch.E. Jl*, **29**, 632.

Owens, D. H., and Raya, A., 1982, *Proc. Instn elect. Engrs*, Pt D, **129**, 298.

Palmor, Z. J., 1980, *Int. J. Control*, **32**, 937; 1985, *A.I.Ch.E. Jl*, **31**, 215.

Palmor, Z. J., and Shinnar, R., 1981, *A.I.Ch.E. Jl*, **27**, 793.

Rivera, D. E., and Morari, M., 1987, *Int. J. Control*, **46**, 505.

Rivera, D. E., Morari, M., and Skogestad, S., 1985, *I. & E.C. Process Des. Dev.*, **25**, 252.

Smith, O. J. M., 1957, *Chem. Engng Prog.*, **53**, 217.

Skogestad, S., and Morari, M., 1986, Control of ill-conditioned plants: high purity distillation. *A.I.Ch.E. Ann. Meeting*, Miami, Florida, U.S.A.